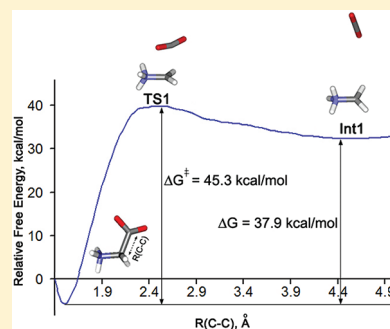


On the Mechanism and Rate of Spontaneous Decomposition of Amino Acids

Anastassia N. Alexandrova^{*,†} and William L. Jorgensen[‡][†]Department of Chemistry and Biochemistry, University of California, Los Angeles, Los Angeles, California 90095-1569, United States[‡]Department of Chemistry, Yale University, New Haven, Connecticut 06520-8107, United States

ABSTRACT: Spontaneous decarboxylation of amino acids is among the slowest known reactions; it is much less facile than the cleavage of amide bonds in polypeptides. Establishment of the kinetics and mechanisms for this fundamental reaction is important for gauging the proficiency of enzymes. In the present study, multiple mechanisms for glycine decomposition in water are explored using QM/MM Monte Carlo simulations and free energy perturbation theory. Simple CO₂ detachment emerges as the preferred pathway for decarboxylation; it is followed by water-assisted proton transfer to yield the products: CO₂ and methylamine. The computed free energy of activation of 45 kcal/mol, and the resulting rate-constant of $1 \times 10^{-21} \text{ s}^{-1}$, can be compared with an extrapolated experimental rate constant of $\sim 2 \times 10^{-17} \text{ s}^{-1}$ at 25 °C. The half-life for the reaction is more than 1 billion years. Furthermore, examination of deamination finds simple NH₃-detachment yielding α -lactone to be the favored route, though it is less facile than decarboxylation by 6 kcal/mol. Ab initio and DFT calculations with the CPCM hydration model were also carried out for the reactions; the computed free energies of activation for glycine decarboxylation agree with the QM/MM result, whereas deamination is predicted to be more favorable. QM/MM calculations were also performed for decarboxylation of alanine; the computed barrier is 2 kcal/mol higher than for glycine in qualitative accord with experiment.



INTRODUCTION

It was recently proposed that decarboxylation of amino acids is among the slowest reactions that exist.¹ A number of studies have shown that, indeed, in spontaneous decomposition of polypeptides, the cleavage of the peptide bond happens substantially more easily than the decomposition of amino acids themselves. For example, decarboxylation of glycine was estimated to have a rate constant of $\sim 2 \times 10^{-17} \text{ s}^{-1}$ at 25 °C and pH 6.8,¹ yielding a half-life of 1.1 billion years, whereas the half-life of alanine decarboxylation, as measured via a radioactive labeling method by Conway and Libby,² is ~ 10 billion years at room temperature. These numbers exceed that of the uncatalyzed hydrolysis of the peptide-bond by many orders of magnitude.^{3–6}

In living organisms, glycine decarboxylation is catalyzed by glycine decarboxylase, a photosynthetic enzyme, intensively studied over the past years.^{7–21} In animals, this reaction happens in the cells of the liver and kidneys. In plants, it is responsible for producing photorespiratory CO₂ in mitochondria, and is thought to contribute to the evolution of the process of photosynthesis. Glycine decarboxylation is coupled to glycine–serine interconversion involving serine hydroxymethyltransferase.^{8,15–18} The reaction can be represented as 2 glycine \rightarrow NH₃ + CO₂ + serine.^{19–21}

The deamination of amino acids has also attracted much attention.^{22–34} Deamination of glycine and alanine is catalyzed by glycine dehydrogenase.²⁴ This protein has been associated with dormant tuberculosis bacteria and their drug-resistance. Multiple early experimental works reported glycine deamination to be exclusively aerobic, which suggested an oxidative mechanism for

the reaction.^{25–27} Oxidative deamination was proposed to yield cyanic acid.²⁸ Glycine oxidase also catalyzes deamination of glycine and other amino acids.^{28,29} Mechanistic study of this enzymatic reaction by Molla et al. showed its reversible nature.²⁹ Glycine is also utilized by many anaerobic bacteria,^{30,31} conveying it in a reductive deamination, yielding acetic acid and ammonia. Of course, hydrolysis of amino acids is carried out by proteolytic enzymes, whereas in neutral or even acidic or basic aqueous solutions, amino acids are remarkably stable. Hydrolysis of glycine can occur under harsh acidic conditions or, for example, under exposure to ultraviolet radiation ($\lambda < 2265 \text{ Å}$).³²

Many catalytic methods have been explored for both decarboxylation and deamination of amino acids. Venkatesh et al.³³ studied the oxidative deamination of (p-sulfophenyl)glycine by molecular oxygen in the presence of the vitamin B₆ coenzyme pyridoxal derivatives and metal ions. The oxidative action of vitamin B₁₂ in glycine deamination has been implicated in the loss of glycine in the bloodstream of children given glycine intravenously.³⁴ Lewis acids, BF₃ and AlCl₃, have also been used as catalysts, and the reactions were found to proceed faster in solvents with high dielectric constants.³⁵ The presence of Ca²⁺ ions and glucagon was shown to increase the rate of glycine degradation by rat liver mitochondria.³⁶ Complexes of Au(III), an ion of known toxicity and carcinogenicity, were found to

Received: August 24, 2011

Revised: September 29, 2011

Published: October 14, 2011

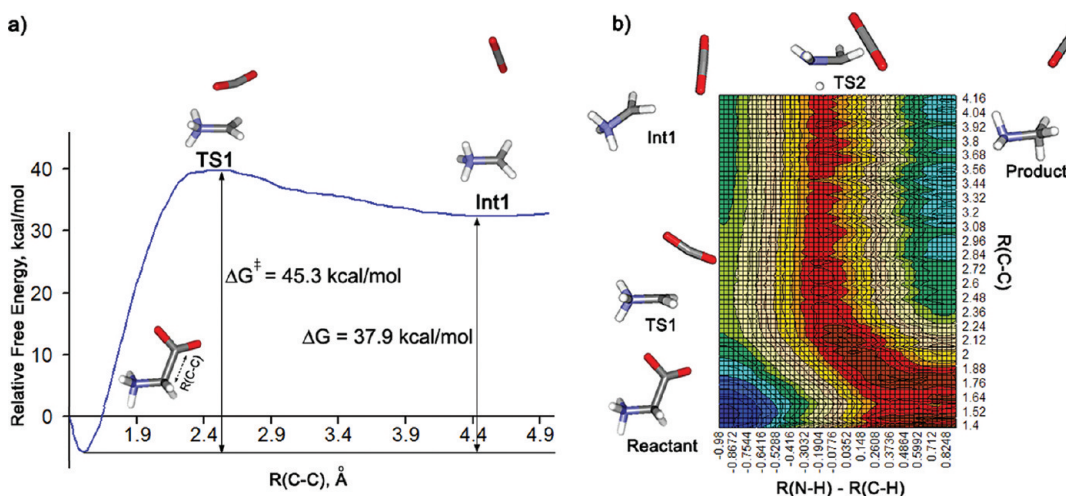


Figure 1. Unassisted decarboxylation of glycine in water: (a) free energy profile from the QM/MM FEP calculations and (b) 2D PMF for decarboxylation accompanied by intramolecular proton transfer.

catalyze deamination and subsequent decarboxylation of glycine.³⁷ Decarboxylation and deamination of glycine in the presence of *N*-bromoacetamide were studied in acidic, basic, and neutral media.³⁸ The reaction exhibited a strong dependence upon the pH of the solution. Oxidative deamination of glycine by O₂ was also studied, and it was shown to be catalyzed by adrenaline, pyrocatechol, hydroxyhydroquinone, and related derivatives.^{39,40} The products are NH₃ and OHCCO₂H with the latter decomposing into CH₂O and CO₂. Reversible oxidative deamination of glycine was detected in the presence of tyrosinase and *p*-cresol.^{41,42} A small amount of ammonia in this process irreversibly recombined with *p*-cresol. Furthermore, nitrous acid (HNO₂) has been shown to induce glycine deamination.⁴³

Reactions of the glycine anion H₂NCH₂CO₂⁻ with various radical species were also found to result in decarboxylation.⁴⁴ The reactions were initiated by oxidation of the amino group, followed by rapid release of CO₂. UV and α -radiation also promote deamination of glycine in solution;^{45,46} the formation of H⁺ or OH⁻ ions or hydrogen peroxide from the solvent appears to be involved. In the presence of ketoglutarates, NaClO₂ causes almost complete deamination of glycine, alanine, and a few other amino acids, and the active role of the forming NaClO was suggested in this case.⁴⁷

Despite much effort to study catalytic decomposition of amino acids, it is unclear how these processes proceed in the absence of catalysis. Elucidation of the associated kinetics and mechanisms are, however, important since the processes are so fundamental and provide a reference for evaluation of the proficiency of degradative enzymes. To this end, the present combined quantum and statistical mechanical (QM/MM) study has been pursued to gain insight into the mechanisms for uncatalyzed decarboxylation and deamination of glycine in aqueous solution. This work follows technically similar QM/MM investigations of decarboxylation of a biotin model and Kemp decarboxylations of benzisoxazoles.⁴⁸ In both cases, the predicted free energies of activation and solvent effects were in excellent agreement with experimental data. The QM/MM approach includes quantum mechanical treatment of the reacting system in the presence of hundreds of explicit solvent molecules. Along the studied reaction paths, the entire system is sampled via Monte Carlo (MC) statistical mechanics in conjunction with free energy perturbation

(FEP) calculations to yield free energies of activation, geometries of transition states, and elucidation of the role of the solvent.

COMPUTATIONAL METHODS

BOSS 4.6 was used for the QM/MM calculations.⁴⁹ The reacting system was treated using the semiempirical molecular orbital method, PDDG/PM3.⁵⁰ PDDG/PM3 has been extensively validated for gas-phase structures and energetics, and it has performed well in QM/MM/MC studies for numerous S_N2, addition, and elimination reactions in solution.^{48,51} The explicit TIP4P water model was used to represent the solvent.⁵² The systems consisted of a QM part with the amino acid and sometimes one or two water molecules placed in a periodic cube of 500 TIP4P water molecules.

The FEP calculations were performed during the Metropolis MC simulations in the NPT ensemble at 25 °C and 1 atm. The energy of the QM region was evaluated for every attempted move of a solute, which occurred every 100 configurations. For the reacting system, all degrees of freedom, except for the reaction coordinates, were sampled, whereas the solvent molecules were treated as rigid bodies possessing only rotational and translational degrees of freedom. For the solute, CM3 charges scaled by a factor of 1.14, which minimizes errors for free energies of hydration,⁵³ were used to calculate the electrostatic portion of the solute–solvent interaction energy. The intermolecular interactions were truncated with feathered spherical cutoffs at 10 Å based on distances between non-hydrogen atoms. The reaction coordinates, typically interatomic distances corresponding to forming or breaking bonds, were perturbed along the reaction route, and the corresponding increments of the free energy were then combined into a free energy profile or “potential of mean force” (PMF) or into a two-dimensional (2D) free-energy map. For 1D PMFs, the reaction coordinate increment was ± 0.02 Å. For 2D PMFs, the initial scanning of the surface was done with an increment of ± 0.04 Å, and the vicinities of stationary points were further refined with an increment of ± 0.02 Å. Each FEP window entailed 2.5×10^6 configurations of equilibration followed by 5.0×10^6 configurations of averaging. The smoothness of the free-energy profiles indicates that the uncertainties in the computed free energies of activation are below 1 kcal/mol. It is worth noting

Table 1. Key Distances (\AA) for Glycine, and the Transition States and Intermediates for Its Decarboxylation from the QM/MM Simulations

	TS1	TS2	TS3	TS4	TS5	TS6
$R(\text{C}-\text{C})$	2.50	3.78	2.48	3.99	3.57	3.62
$R(\text{C}-\text{H})^a$		1.51	3.77	2.22	1.24	1.11
$R(\text{N}-\text{H})^b$		1.49	1.01	0.96	1.04	1.41
$R(\text{O}-\text{H})_1^c$			0.96	0.96	1.18	2.58
$R(\text{O}-\text{H})_2^c$			1.88	1.83	1.83	1.49
glycine Int1 Int2 ^d Int3 Int4 ${}^+ \text{H}_3\text{NCH}_2 + \text{OH}^- \text{H}_2\text{NCH}_2 + \text{H}_2\text{O}$						
$R(\text{C}-\text{C})$	1.50	4.44	4.34	3.98	3.51	3.57
$R(\text{C}-\text{H}1)$		2.52	1.44		1.08	1.12
$R(\text{N}-\text{H}2)$		1.01	1.05		1.06	1.83
$R(\text{O}-\text{H}1)$		1.02	1.06		2.86	3.56
$R(\text{O}-\text{H}2)$		1.75	1.82		1.74	0.97

^a C–H distance from C to the H that arrives to C. ^b N–H distance from N to the H that it loses. ^c $R(\text{O}-\text{H})_1$ is the distance from O of H_2O to the H donated to CH_2 ; $R(\text{O}-\text{H})_2$ is the distance from O of H_2O to the H received from N. ^d Geometry of Int2 as obtained from the 2D PMF (Figure 2b).

more than 100 billion single-point QM calculations were executed for this study. Thus, use of an efficient semiempirical molecular orbital method such as PDDG/PM3 was essential.

RESULTS AND DISCUSSION

Unassisted Decarboxylation. The first mechanism to be studied was direct detachment of CO_2 from glycine zwitterion. The resultant free-energy profile is shown in Figure 1a using the C–C distance as the reaction coordinate. Some structural details for transition states and intermediates for the decarboxylation reactions are given in Table 1. At a C–C separation of 2.50 \AA , the system crosses a transition state, TS1, with a free energy of activation (ΔG^\ddagger) of 45.3 kcal/mol. The initial products are the ylide ${}^+ \text{H}_3\text{NCH}_2^-$ and CO_2 , which are 37.9 kcal/mol higher in free energy at a C–C distance of 4.44 \AA than glycine. PDDG/PM3 optimizations with implicit GB/SA hydration⁵⁴ were also carried out; they yield an overall energetic change of +44.8 kcal/mol, which is consistent with the +37.9 kcal/mol in Figure 1. This “energetic change” is not identical to a free energy change as it is obtained as the difference in heats of formation plus free energies of hydration of the reactant and products. Geometry optimizations using PDDG/PM3 with and without GB/SA hydration also predict that the ylide is 42 and 37 kcal/mol less favorable than its isomer, methylamine, in the gas phase and in water, respectively. Thus, rearrangement of the ylide Int1 to methylamine or its protonation to yield protonated methylamine is expected to complete the reaction.

The rearrangement of Int1 in conjunction with the decarboxylation was investigated. It can happen either after the decarboxylation step or simultaneously with it and can be assisted by a water molecule, serving as a relay between the proton donor and acceptor. The unassisted reaction is considered first. A 2D PMF was built, coupling the C–C bond cleavage to the proton shift (Figure 1b). The first reaction coordinate was chosen, as before, as the C–C distance. The second reaction coordinate was the difference between $R(\text{N}-\text{H})$ for H-departure from the NH_3^+ group and $R(\text{C}-\text{H})$ for H-arrival on the CH_2^- , $\{R(\text{N}-\text{H}) - R(\text{C}-\text{H})\}$.

The sum of the two distances, $\{R(\text{N}-\text{H}) + R(\text{C}-\text{H})\}$, was fixed. The magnitude of the sum was determined from two separate 2D PMFs for the proton transfer only, where $R(\text{N}-\text{H})$ and $R(\text{C}-\text{H})$ were the reaction coordinates. One such map was built with $R(\text{C}-\text{C})$ fixed at 2.50 \AA , as in the transition state, TS1, and the other was built with $R(\text{C}-\text{C})$ being greater than 3 \AA at the beginning of the simulation, and sampled freely thereafter (i.e., in the Int1 plus CO_2 region). The sum, $\{R(\text{N}-\text{H}) + R(\text{C}-\text{H})\}$, was observed to be similar between the two runs, and hence, it was set at 2.90 \AA . This approach with a combined reaction coordinate for the H-transfer has been validated previously.^{52f,56}

From the 2D PMF shown in Figure 1b, the reaction is found to proceed stepwise. The C–C bond cleaves first via the transition state TS1, as in Figure 1a. The ΔG^\ddagger for this step is 45.8 kcal/mol, in close agreement with the results in Figure 1a. The forming Int1 then undergoes the proton shift through the transition state TS2 yielding methylamine. Not surprisingly, after the CO_2 is released, the barrier for the proton transfer step is largely independent of the C–C separation. The free-energy barrier is about 45.3 kcal/mol for $R(\text{C}-\text{C}) > 3.2 \text{\AA}$, making the proton transfer the rate-determining step. It is formally a “forbidden” 4-electron process according to the Woodward–Hoffmann rules. The overall ΔG^\ddagger for the C–C cleavage plus intramolecular proton transfer is then 85.2 kcal/mol. This value is conceptually unreasonable and inconsistent with the experimental data, which indicates a ΔG^\ddagger of ca. 40 kcal/mol.¹ Thus, an alternative mechanism was pursued.

Decarboxylation Assisted by One Water Molecule. The rearrangement of Int1 can be assisted through the inclusion of one water molecule as a relay between the proton donor (NH_3^+) and acceptor (CH_2^-) groups. The QM region now consists of the glycine zwitterion and one water molecule (Figure 2). The FEP calculations for the decarboxylation step in this case yielded essentially the same activation barrier as in Figure 1a. No specific participation of the included water molecule is apparent. The transition states TS1 and TS3 are basically identical. The ylide Int2 appears to be a true minimum on the free energy surface; it does not undergo a spontaneous proton transfer involving the quantum water molecule. Therefore, as in the previous case, the proton transfer for the intermediate, Int2, follows decarboxylation, and can be considered separately.

From pK_a considerations, protonation of the CH_2^- group by H_2O is expected to be more favorable than deprotonation of the NH_3^+ group, so the former process was considered first. A full free-energy map was computed for the process with the reaction coordinates as $R(\text{C}-\text{H})$ and $R(\text{O}-\text{H})$. As reflected in Figure 2b, it was found that the O to C proton transfer appears to occur in two stages. First, there is a barrier of only 1.3 kcal/mol (TS4), resulting in a shallow minimum for the intermediate Int3, which is 13.4 kcal/mol lower in free energy than Int2. In Int3, the OH and CH_2 groups share the transferring proton H1 in what may be viewed as a hydrogen bond (Figure 2b and Table 1). The proton transfer is then completed via a second low barrier (TS5) to form the methyl ammonium - hydroxide ion pair Int4. The overall O to C proton transfer is highly exoergic with Int4 42 kcal/mol lower in free energy than the ylide Int2. It may be noted that, in this case, the sum, $\{R(\text{O}-\text{H}) + R(\text{C}-\text{H})\}$, is not constant throughout the reaction, and the reaction follows a distinctly stepwise path.

Finally, the ammonium group can be deprotonated by the hydroxide ion. Such proton transfers have been investigated

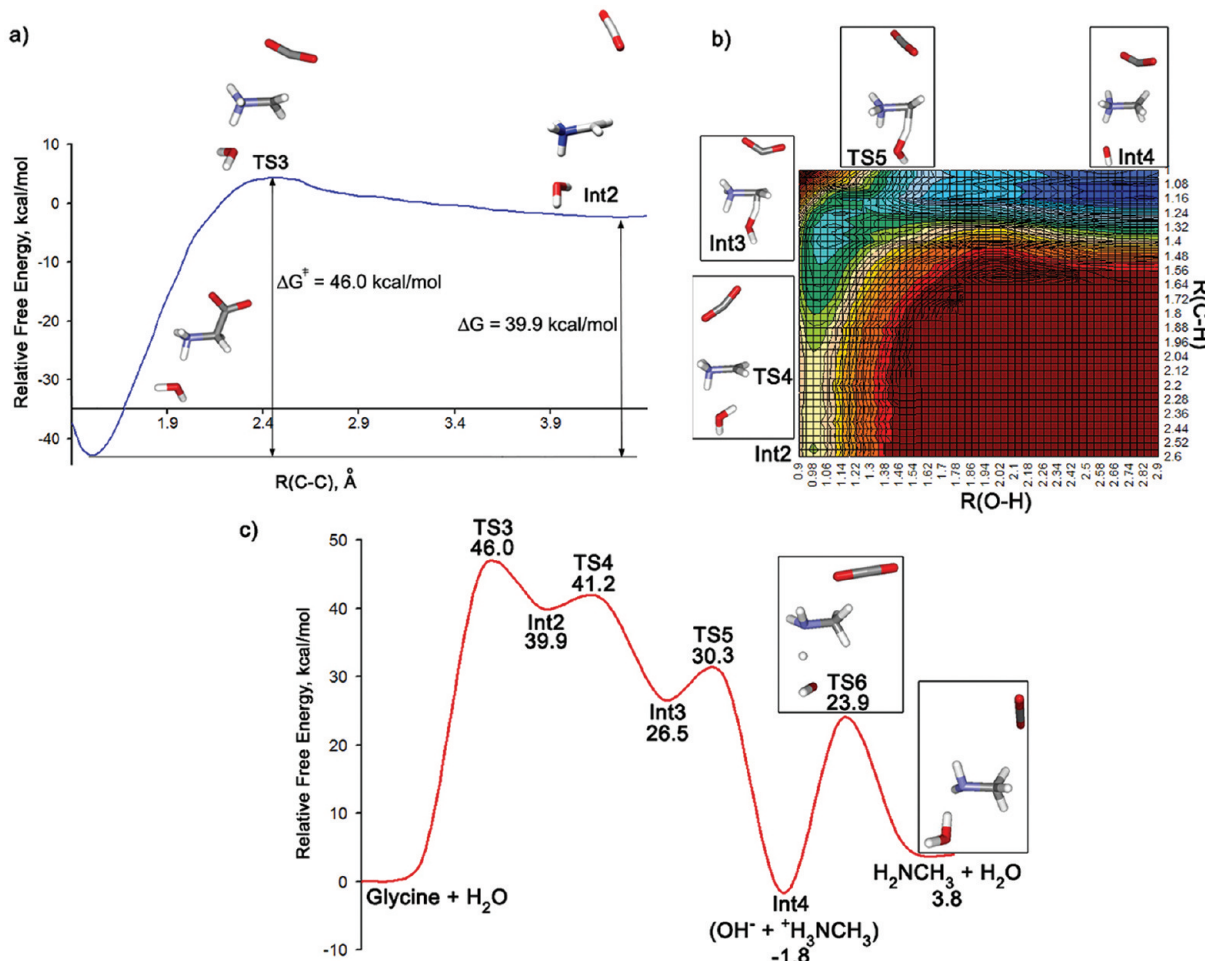


Figure 2. QM/MM results for decarboxylation of glycine assisted by one water molecule: (a) free energy profile for the decarboxylation step, (b) 2D PMF for protonation of CH_2^- , and (c) overall reaction profile.

previously, and it has been shown that they do adhere to the approximation that $\{R(\text{N}-\text{H}) + R(\text{O}-\text{H})\}$ should be constant.⁵⁵ Therefore, the dimensionality of the problem can be reduced, and the process can be described by a 1D PMF. The FEP calculations yielded a ΔG^\ddagger of 25.7 kcal/mol passing through **TS6** to yield methylamine and a water molecule. This barrier might be overestimated due to the imposed constraint on the sum of $R(\text{O}-\text{H})$ and $R(\text{N}-\text{H})$. However, this step is far from rate-determining because **TS6** is 22.1 kcal/mol below **TS3** in free energy. In fact, there may be alternative pathways for the conversion of the ylide **Int2** to the products, but the present results demonstrate that there is at least one pathway that involves no additional activation beyond formation of **TS3** or equivalently **TS1**.

The overall reaction profile for glycine decarboxylation assisted by one water molecule is given in Figure 2c. The simple detachment of CO_2 from the glycine zwitterion is the first and rate-limiting step for the reaction. The computed ΔG^\ddagger of 45.3 (TS1) or 46.0 (TS3) kcal/mol translate to a rate constant for the reaction of ca. $1 \times 10^{-21} \text{ s}^{-1}$, which is somewhat slower than the experimental estimate of ca. $2 \times 10^{-17} \text{ s}^{-1}$ at 25 °C based on rate data measured at 170–260 °C.¹ Also in Figure 2c, the methylamine product complex ends up 5.6 kcal/mol higher in free energy than the **Int4** ion pair. The difference should be reduced by ca. 2 kcal/mol for a cratic correction corresponding to 1 M

standard states for the ion pair.⁵⁶ However, the favoring of the ion pair is still overestimated based on known pK_a values for methylamine (10.7) and water (15.7), which imply that the free energy change for $\text{CH}_3\text{NH}_2 + \text{H}_2\text{O} \rightarrow \text{CH}_3\text{NH}_3^+ + \text{OH}^-$ should be +6.8 kcal/mol. The achievement of high accuracy for such computations is challenging owing to the large constituent terms for the bond making, bond breaking and solvation changes.

Unassisted Deamination. Deamination of glycine was also examined using $R(\text{C}-\text{N})$ as a reaction coordinate. First, the 1D PMF was constructed, which revealed that the products of the reaction are α -lactone and ammonia. The zwitterion $^+\text{H}_2\text{CCH}_2\text{COO}^-$ from a possible $S_{\text{N}}1$ process is not formed as an intermediate. This indicated that at least two reaction coordinates are required for a proper assessment of the energetics and mechanism, $R(\text{C}-\text{N})$ for NH_3 departure and $\angle(\text{C}-\text{C}-\text{O})$ for the formation of α -lactone. However, the reaction map resulting from this pair in the absence of further geometric constraints led to some intermediates with unreasonable geometries. Therefore, a dihedral angle for the carboxyl group ($\text{N}-\text{C}\alpha-\text{C}-\text{O}$) was fixed at 180°. Since this value is what is expected for the glycine zwitterion and transition state, the constraint is expected to have little effect on the computed activation barrier and reaction path. The resultant 2D PMF is presented in Figure 3.

It can be seen from the map that the new C–O bond begins to form earlier than the C–N bond cleaves. The reaction proceeds

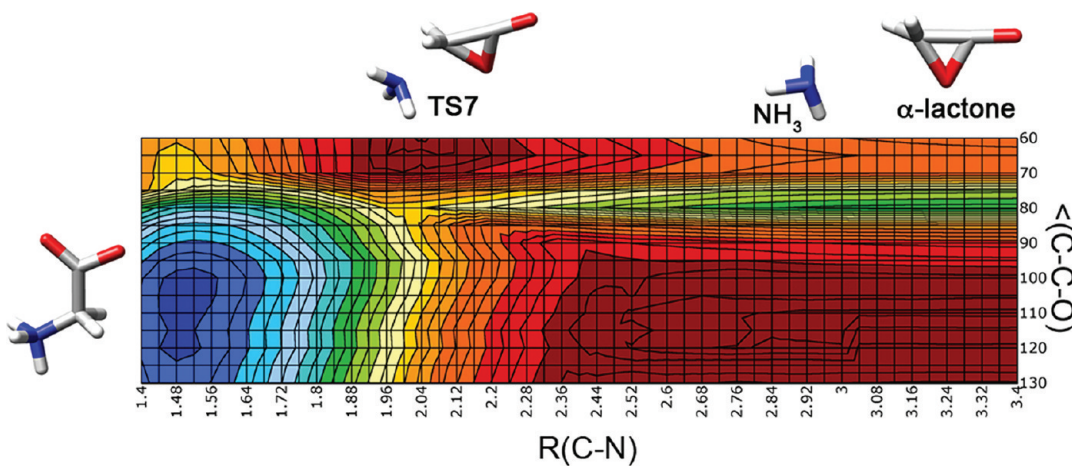


Figure 3. QM/MM free-energy map for unassisted deamination of glycine in aqueous solution resulting in α -lactone and ammonia.

Table 2. Ab Initio and DFT Results for the Direct Decarboxylation and Deamination Transition States Including CPCM Hydration

decarboxylation TS		
	MP 2/6-311+G*	B3LYP/6-311++G**
ΔG^\ddagger , kcal/mol	42.8	44.5
$R(C_1-C_2)$, Å	4.32	4.27
$R(C_1-N)$, Å	1.54	1.53
$\angle(N-C_1-C_2)$, deg	65.4	67.1
$R(C_2-O_1)$, Å	1.17	1.16
$R(C_2-O_2)$, Å	1.17	1.16
ω_1 , cm ⁻¹	34.8i (34)	27.8i (30)
deamination TS		
	MP 2/6-311+G*	B3LYP/6-311++G**
ΔG^\ddagger , kcal/mol	37.4	37.0
$R(C_1-N)$, Å	2.33	2.55
$R(C_1-O_1)$, Å	1.74	1.70
$R(C_2-O_1)$, Å	1.30	1.30
$R(C_2-O_2)$, Å	1.22	1.20
ω_1 , cm ⁻¹	359.4i (668) ^a	231.1i (379) ^a

^a Infrared intensities are given in parentheses.

via TS7, in which $R(C-N) = 2.02 \text{ \AA}$, and $\angle(C-C-O) = 82^\circ$. The process can be viewed as an internal S_N2 reaction yielding NH_3 and α -lactone. The computed free energy barrier for the deamination is 50.6 kcal/mol, which is higher than the computed barrier to the decarboxylation and the experimentally predicted value for spontaneous decomposition of glycine.¹ The products of the reaction are 30.9 kcal/mol higher in free energy than the glycine zwitterion. Subsequent hydrolysis of α -lactone would be expected.

Ab Initio and DFT Results for the Unassisted Processes. The transition states for the direct decarboxylation and deamination were also located using the density functional method, B3LYP,⁵⁷ with the 6-311++G** basis set⁵⁸ and MP2/6-311+G*.⁵⁹ The effects of hydration were included via the implicit CPCM solvation model.⁶⁰ Table 2 summarizes the computed

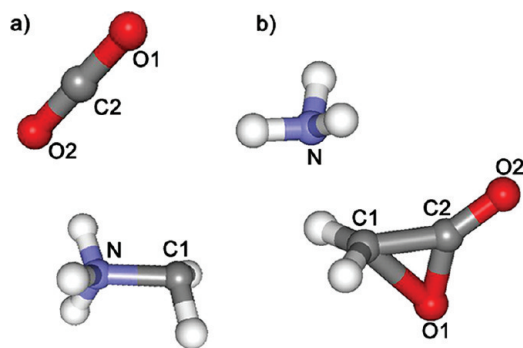


Figure 4. Transition states for glycine (a) decarboxylation and (b) deamination found with the DFT and ab initio calculations. Bond lengths and angles are listed in Table 2.

molecular parameters and activation free energies, and Figure 4 illustrates the computed transition states. For decarboxylation, the transition state analogous to TS1 (or TS3) was found by both methods. The only imaginary frequency corresponds to the C_1-C_2 stretching motion for the CO_2 detachment. The $C-C$ distance in this TS is significantly larger than that yielded by QM/MM simulations. In order to confirm that the correct TS was found, we performed the full scans along $R(C-C)$, from the Gly zwitterions to the products, at both levels of theory. We found that the ab initio potential energy surface is very flat, starting $R(C-C) = 2.8 \text{ \AA}$, and so location and even existence of the true stationary point becomes questionable. In accord with the topography of the potential energy surface, the found imaginary frequency is quite low. The ΔG^\ddagger values for decarboxylation are in accord between the QM/MM, DFT, and MP2 calculations. For deamination, both B3LYP and MP2 predict the existence of a transition state corresponding to NH_3 -detachment from the glycine zwitterion, analogous to TS7 (Figure 3). The C_1-N stretch is the normal mode corresponding to the only imaginary frequency found in this species (Table 2). However, the activation free energy for deamination is lower than that predicted by the QM/MM FEP/MC simulations. It is also lower than the QM/MM, DFT, and MP2 results for the decarboxylation. Although there are uncertainties in the accuracy of the CPCM model as well as the PDDG/PM3 calculations, the

experimental observation is that glycine decomposition occurs by decarboxylation in accord with the QM/MM results.¹

Deamination by Hydrolysis. The deamination of glycine zwitterion could also be conceived to occur in a hydrolytic fashion; a water molecule acts as a nucleophile attacking the C_α carbon atom and displacing the leaving group, ammonia. Decarboxylation in an analogous manner is nonsensical as the products would be H₃NCH₂OH₂²⁺ and CO₂²⁻.

The possible deamination was modeled by including a water molecule in the QM region, and the distance from its oxygen atom to C_α R(C—O), and R(C—N) were used as the reaction coordinates to generate a 2D PMF (Figure 5). From the map, the reaction is found to proceed in a concerted fashion. In the transition state, TS8, the C—O bond formation is well advanced, whereas the NH₃ departure is still in progress. The activation barrier of this hydrolytic path (154 kcal/mol) is unreasonable. It embodies penalties for being both an S_N2 process with a weak nucleophile and for poorer solvation of the more charge delocalized transition state than reactants. The product of the reaction shown in Figure 5 would further undergo additional protonation and deprotonation events, which are not considered here.

Hydrolysis Accompanied by Deprotonation of the Nucleophilic H₂O. In view of the weak nucleophilicity of a water

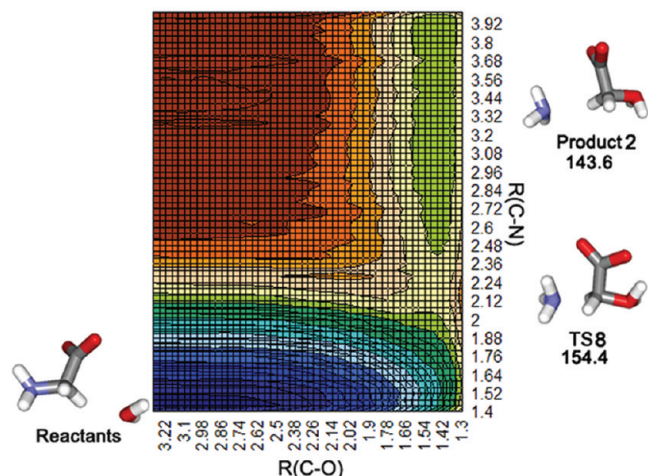


Figure 5. QM/MM free-energy map for the hydrolytic deamination of glycine.

molecule, an alternative mechanism can be imagined, in which the nucleophilic attack by H₂O would be accompanied by its deprotonation. The most obvious proton acceptor in the system is one of the oxygen atoms of the negatively charged carboxylate group. An attempt was made to construct a 2D PMF using R(C—O) as the reaction coordinate for the nucleophilic attack and {R(O_w—H) — R(O_{C=O}—H)} as the reaction coordinate for proton transfer. The reaction was found to follow a stepwise mechanism, with proton transfer occurring first and being completely uncoupled from the nucleophilic attack. Therefore, the proton transfer step was considered separately. During it, the system crosses the first transition state, TS9, resulting in the intermediate, Int5 (Figure 6). Int5 is a complex of protonated glycine and a hydroxide ion, and it is 7.0 kcal/mol higher in energy than the initial glycine–water adduct. This seems reasonable in view of the difference in pK_a values for water and a carboxylic acid, formation of the E conformer of the acid, and the hydrogen bonding in the product.

Most conceivably, after the protonation of the carboxyl group, an S_N2 reaction occurs with OH[−] as the nucleophile displacing NH₃ from the protonated glycine. When R(C—O) and R(C—N) as the reaction coordinates were used, the 2D PMF was built for this pathway (Figure 6a). From the map, the reaction starts from the attack on C_α, and the system subsequently releases NH₃. However, the overall activation free energy barrier to this reaction is very high; the overall reaction profile is shown in Figure 6b. A major problem in this case is the poorer free energy of solvation for the neutral Product3 than for the starting zwitterion or the Int5 ion pair. The H⁺ transfer from COOH to NH₃ would complete this reaction. However, this hydrolytic mechanism is clearly not competitive due to the high free energy barrier. For such a pathway to be more competitive, much more elaborate proton transfer sequences could also be involved such that the leaving group, NH₃, becomes protonated and the protonated carboxylate group is deprotonated as the nucleophilic attack progresses.

Hydrolysis Assisted by One Water Molecule. The nucleophilic water molecule can also be deprotonated by another water molecule (Figure 7). Using R(C—O_{w1}) as the reaction coordinate for the attack and {R(O_{w1}—H) — R(O_{w2}—H)} as the reaction coordinate for the proton transfer, the 2D PMF was built for this reaction. From the 2D PMF, it follows that autoionization of water happens first, independent of the nucleophilic attack.

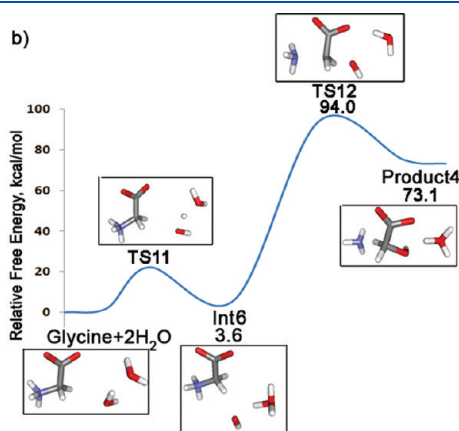


Figure 6. Hydrolysis accompanied by the proton transfer from the nucleophilic H₂O to the carboxylate group: (a) 2D PMF for the nucleophilic attack and NH₃ departure and (b) the full reaction profile, including proton transfer and the attack accompanied by the loss of NH₃.

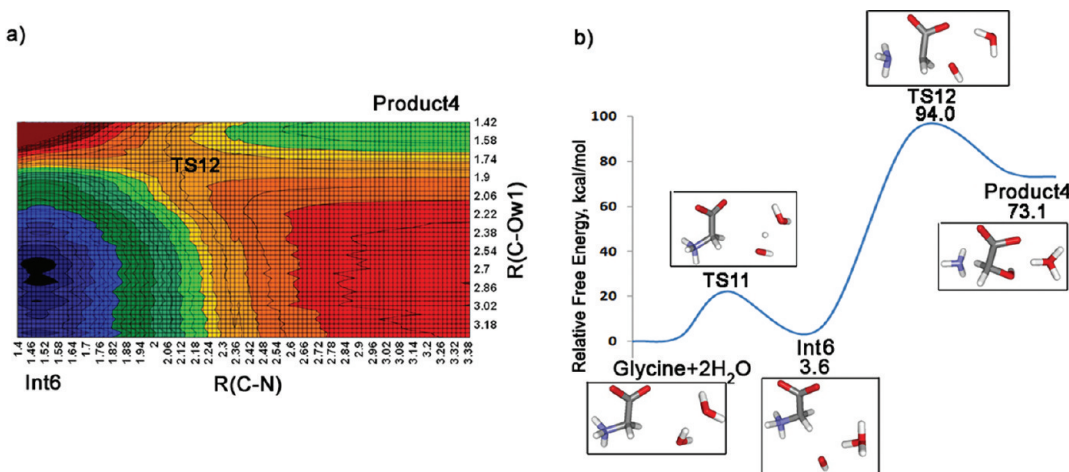


Figure 7. QM/MM results for hydrolytic deamination assisted by autoionization of H_2O : (a) 2D PMF for the nucleophilic attack and NH_3 departure (second step) and (b) the full reaction profile.

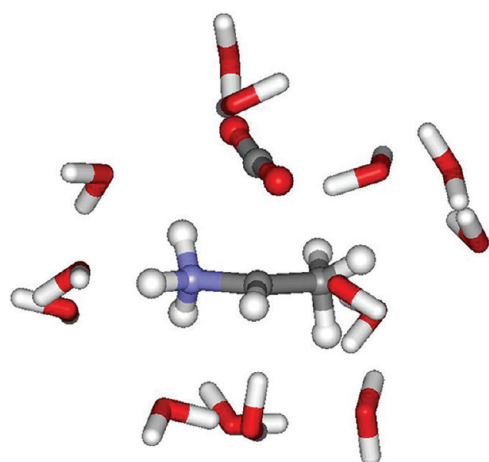


Figure 8. Transition state toward decarboxylation of Ala, from QM/MM FEP MC simulations. The solvent water molecules found within 3 Å from the solute are shown. Notice the rather unstructured solvation pattern around the CH group acquiring the negative charge.

The system crosses the transition state, **TS11**, yielding $\text{OH}^- \cdot \text{H}_3\text{O}^+$ complexed to the glycine molecule in the intermediate, **Int6**. The formation of **Int6** is 3.6 kcal/mol higher in free energy than that of the initial complex (Figure 7b).

Then, the nucleophilic attack by the formed hydroxide ion can be accompanied by NH_3 departure. A 2D PMF (shown in Figure 7a) was built for this process with $R(\text{C}-\text{O}_{\text{w}1})$ and $R(\text{C}-\text{N})$ as reaction coordinates. The reaction follows a single-step mechanism. OH^- attacks C_α early in the route. The molecule then loses ammonia, yielding the high-energy **Product4** (Figure 7a). The overall reaction profile is given in Figure 7b. Again subsequent or simultaneous proton transfers would be expected to complete the reaction. In their absence, glycine decomposition is unlikely to involve displacement of ammonia by hydroxide ion generated by autoionization of water.

Decarboxylation of Alanine. The QM/MM approach was then applied to the direct decarboxylation of the alanine zwitterion (Figure 8). The computed activation barrier, 47.1 kcal/mol, and C–C distance at the transition state, 2.52 Å, can

be compared to the corresponding values for glycine, 45.3 kcal/mol and 2.50 Å. The pattern is consistent with the observed, significantly longer half-life for alanine.^{1,2} One contributor to the difference in ΔG^\ddagger for Gly and Ala could be destabilization from the electron-donating CH_3 group of the Ala side chain to the anionic portion of the zwitterionic product and intervening transition state. This is supported by the fact that the isodesmic reaction, $\text{NH}_3\text{CH}_2 + \text{CH}_3\text{CH}_3 \rightarrow \text{NH}_3\text{CHCH}_3 + \text{CH}_4$, is exothermic with $\Delta E = -2.7$ kcal/mol at the B3LYP/6-311++G** level. Additionally, poorer solvation of NH_3CHCH_3 and the transition state leading to it (Figure 8) compared to the less-hindered NH_3CH_2 could also contribute to the higher barrier for decarboxylation of the alanine zwitterion.

CONCLUSIONS

The present study provides insights into the mechanism and energetics of a fundamental biochemical reaction, spontaneous decomposition of glycine. The present QM/MM statistical mechanical investigation finds that the most likely pathway for decomposition of glycine in aqueous solution occurs via direct decarboxylation. CO_2 departure is the first and the rate-determining step of the reaction, and it does not require any assistance from the solvent water. The resultant ammonium ylide would be expected to undergo simultaneous or subsequent rearrangement to methylamine or protonation to yield protonated methylamine. The computed activation free energy of 45–46 kcal/mol is in good agreement with results of DFT and MP2 calculations with the CPCM continuum hydration model and in reasonable range of the experimentally estimated activation enthalpy of 39 ± 2 kcal/mol.¹ All deamination and hydrolytic routes of glycine decomposition were found to be noncompetitive. Direct deamination is computed to occur via an internal $\text{S}_{\text{N}}2$ mechanism yielding ammonia and α -lactone. The free energy of activation in this case from the QM/MM calculations is 50.6 kcal/mol, whereas the barriers from the DFT/CPCM and MP2/CPCM calculations appear to be too low. Hydrolytic mechanisms have activation energies greater than 70 kcal/mol. Decarboxylation of alanine was also investigated; the barrier height is predicted to increase by ca. 2 kcal/mol as compared to that for glycine, in agreement with the available experimental data.

AUTHOR INFORMATION

Corresponding Author

*E-mail: ana@chem.ucla.edu.

ACKNOWLEDGMENT

Gratitude is expressed to the National Science Foundation (CHE-0446920), the National Institutes of Health (GM032136), and the University of California (Faculty Career Development Award to ANA) for support of this work and to Prof. Richard Wolfenden for discussions.

REFERENCES

- (1) Snider, M. J.; Wolfenden, R. *J. Am. Chem. Soc.* **2000**, *122*, 11507–11508.
- (2) Conway, D.; Libby, W. F. *J. Am. Chem. Soc.* **1958**, *80*, 1077–1080.
- (3) Abelson, P. H. *Sci. Am.* **1956**, *195*, 83–91.
- (4) Kahne, D.; Still, W. C. *J. Am. Chem. Soc.* **1988**, *110*, 7529–7534.
- (5) Bryant, R. A. R.; Hansen, D. E. *J. Am. Chem. Soc.* **1996**, *118*, 5498–5499.
- (6) Radzicka, A.; Wolfenden, R. *J. Am. Chem. Soc.* **1996**, *118*, 6105–6109.
- (7) Bauwe, H.; Kolukisaoglu, U. *J. Exp. Botany* **2003**, *54*, 1523–1535.
- (8) Rawsthorne, S.; Douce, R.; Oliver, D. *Soc. Exp. Biol. Semin. Ser.* **1995**, *56*, 87–109.
- (9) Tcherkez, G. *Func. Plant Biol.* **2006**, *33*, 911–920.
- (10) (a) Hausler, R. E.; Lea, P. J.; Leegood, R. C. *Planta* **1994**, *194*, 418–35. (b) Hausler, R. E.; Blackwell, R. D.; Lea, P. J.; Leegood, R. C. *Planta* **1994**, *194*, 406–417.
- (11) Devi, M. T.; Raghavendra, A. S. *Photosyn. Res.* **1993**, *38*, 177–184.
- (12) Hiraga, K.; Kikuchi, G. *J. Biochem. (Tokyo, Japan)* **1982**, *92*, 937–944.
- (13) Klein, S. M.; Sagers, R. D. *Biol. Chem.* **1966**, *241*, 206–209.
- (14) (a) Higara, K.; Kikuchi, G. *Biol. Chem.* **1980**, *255*, 11671–11676. (b) Kikuchi, G. *Mol. Cell. Biochem.* **1973**, *1*, 169–186. (c) Sagers, R. D.; Gunsalus, J. C. *J. Bacteriol.* **1961**, *81*, 541–549.
- (15) Cetin, I.; Fennessey, P. V.; Quick, A. N., Jr.; Marconi, A. M.; Meschia, G.; Battaglia, F. C.; Sparks, J. W. *Am. J. Physiol.* **1991**, *260*, E371–E378.
- (16) Zieske, L. R.; Davis, L. *J. Biol. Chem.* **1983**, *258*, 10355–10359.
- (17) Shingles, R.; Woodrow, L.; Grodzinski, B. *Plant Physiol.* **1984**, *74*, 705–710.
- (18) Walton, N. J.; Woolhouse, H. W. *Planta* **1986**, *167*, 119–128.
- (19) Kikuchi, G. *Mol. Cell. Biochem.* **1973**, *1*, 169–187.
- (20) Yoshida, T.; Kikuchi, G. *J. Biochem.* **1972**, *72*, 1503–1516.
- (21) Roswell, E. V.; Al-Naama, M. M.; Rowsell, K. V. *Biochem. J.* **1982**, *204*, 313–321.
- (22) Frearson, W. R.; Montgomery, E. G. *Biochem. J.* **1924**, *18*, 576–582 and references therein.
- (23) Zeller, E. A. *Helv. Chim. Acta* **1938**, *21*, 880–890.
- (24) Usha, V.; Jayaraman, R.; Toro, J. C.; Hoffner, S. E.; Das, K. S. *Can. J. Microbiol.* **2002**, *48*, 7–13.
- (25) Stephenson, M.; Gale, E. F. *Biochem. J.* **1937**, *31*, 1316–1322.
- (26) Janke, A.; Tayenthal, W. *Biochem. Z.* **1937**, *289*, 76–86.
- (27) (a) Metzler, D. E.; Snell, E. E. *J. Biol. Chem.* **1952**, *198*, 353–361. (b) Ikawa, M.; Snell, E. E. *J. Am. Chem. Soc.* **1954**, *76*, 4900–4902. (c) Hill, M.; Mann, P. J. G. *Biochem. J.* **1966**, *99*, 454–468.
- (28) Nishiyama, Y.; Imanaka, T. *FEBS Lett.* **1998**, *438*, 249–256.
- (29) Molla, G.; Motteran, L.; Job, M.; Pilone, M. S.; Pollegioni, L. *Eur. J. Biochem.* **2003**, *270*, 1474–1482.
- (30) (a) Stadtman, T. S.; Elliott, P.; Tiemann, L. *J. Biol. Chem.* **1958**, *231*, 961–973. (b) Stadtman, T. S.; Elliott, P. *J. Am. Chem. Soc.* **1956**, *78*, 2020–2021.
- (31) Kohlstock, U.-M.; Rücknagel, K. P.; Reuter, M.; Schiethorn, A.; Andreesen, J. R.; Söhling, B. *Eur. J. Biochem.* **2001**, *268*, 6417–6425.
- (32) Weizmann, Ch.; Bergmann, E.; Hirshberg, Y. *J. Am. Chem. Soc.* **1936**, *58*, 1675–1678 and references therein.
- (33) Venkatesh, M. S.; Arthur, E. M. *J. Am. Chem. Soc.* **1991**, *113*, 6479–6487.
- (34) Donnasibilla, L. B.; Olivii, O. *Acta Vitaminol.* **1952**, *6*, 6–9.
- (35) Saiprakash, P. K.; Rajanna, K. C.; Devi, Y. U. *Ind. J. Chem. B* **1984**, *23B*, 646–649.
- (36) Jois, M.; Ewart, S. H.; Brosnan, J. T. *Biochem. J.* **1992**, *283*, 3435–3439.
- (37) Zou, J.; John, G.; Parkinson, J. A.; Chen, Yu.; Sadler, P. *Chem. Commun.* **1999**, 1359–1360.
- (38) Reddy, M. K.; Reddy, C. S.; Sundaram, E. V. *Ind. J. Chem. A* **1984**, *23A*, 197–199.
- (39) Berrenscheen, H. K.; Danzer, W. Z. *Physiol. Chem.* **1933**, *220*, 57–60.
- (40) Kisch, B.; Schuwirth, K. *Biochem. Z.* **1993**, *257*, 89–94.
- (41) (a) Hubbard, S. S. *J. Biol. Chem.* **1938**, *126*, 489–492. (b) Hubbard, S. S. *J. Am. Chem. Soc.* **1939**, *61*, 752–753.
- (42) Pugh, C. E. M.; Raper, H. S. *Biochem. J.* **1927**, *21*, 1370–1383.
- (43) Austin, A. T. *J. Chem. Soc.* **1950**, 149–150.
- (44) Bonifacíć, M.; Štefanić, I.; Hug, G. L.; Armstrong, D. A.; Asmus, K.-D. *J. Am. Chem. Soc.* **1998**, *120*, 9930–9940.
- (45) Voeikov, V. L.; Baskakov, I. V.; Kafkalas, K.; Naletov, V. I. *Bioorg. Khim.* **1996**, *22*, 39–47.
- (46) Dale, W. M.; Davis, J. V.; Gilbert, C. W. *Biochem. J.* **1949**, *45*, 543–546.
- (47) Wieland, T.; Vogelbach, C.; Bielig, H. *J. Ann.* **1948**, *561*, 116–123.
- (48) (a) Acevedo, O.; Jorgensen, W. L. *J. Org. Chem.* **2006**, *71*, 4896–4902. (b) Acevedo, O.; Jorgensen, W. L. *J. Am. Chem. Soc.* **2005**, *127*, 8829–8834.
- (49) Jorgensen, W. L.; Tirado-Rives, J. *J. Comput. Chem.* **2005**, *26*, 1689–1700.
- (50) (a) Repasky, M. P.; Chandrasekhar, J.; Jorgensen, W. L. *J. Comput. Chem.* **2002**, *23*, 1601–1622. (b) Tubert-Brohman, I.; Guimarães, C. R. W.; Repasky, M. P.; Jorgensen, W. L. *J. Comput. Chem.* **2003**, *25*, 138–150.
- (51) (a) Vayner, G.; Houk, K. N.; Jorgensen, W. L.; Brauman, J. I. *J. Am. Chem. Soc.* **2004**, *126*, 9054–9058. (b) Acevedo, O.; Jorgensen, W. L. *Org. Lett.* **2004**, *6*, 2881–2884. (c) Acevedo, O.; Jorgensen, W. L. *J. Am. Chem. Soc.* **2005**, *127*, 8829–8834. (d) Acevedo, O.; Jorgensen, W. L. *J. Am. Chem. Soc.* **2006**, *128*, 6141–6146. (e) Acevedo, O.; Jorgensen, W. L. *J. Org. Chem.* **2006**, *71*, 4896–4902. (f) Alexandrova, A. N.; Jorgensen, W. L. *J. Phys. Chem. B* **2007**, *111*, 720–730.
- (52) (a) Jorgensen, W. L.; Chandrasekhar, J.; Madura, J. D.; Impey, W.; Klein, M. L. *J. Chem. Phys.* **1983**, *79*, 926–935. (b) Jorgensen, W. L.; Jenson, C. J. *Comput. Chem.* **1998**, *19*, 1179–1186.
- (53) Udier-Blagovic, M.; Morales de Tirado, P.; Pearlman, S. A.; Jorgensen, W. L. *J. Comput. Chem.* **2004**, *25*, 1322–1332.
- (54) Jorgensen, W. L.; Ulmschneider, J. P.; Tirado-Rives, J. *J. Phys. Chem. B* **2004**, *108*, 16264–16270.
- (55) Tubert-Brohman, I.; Acevedo, O.; Jorgensen, W. L. *J. Am. Chem. Soc.* **2006**, *128*, 16904–16913.
- (56) Hermans, J.; Wang, L. *J. Am. Chem. Soc.* **1997**, *119*, 2707–2714.
- (57) (a) Parr, R. G.; Yang, W. *Density-functional theory of atoms and molecules*; Oxford University Press: Oxford, U.K., 1989. (b) Becke, A. D. *J. Chem. Phys.* **1993**, *98*, 5648–5652. (c) Perdew, J. P.; Chevary, J. A.; Vosko, S. H.; Jackson, K. A.; Pederson, M. R.; Singh, D. J.; Fiolhais, C. *Phys. Rev. B* **1992**, *46*, 6671–6687.
- (58) (a) Clark, T.; Chandrasekhar, J.; Spitznagel, G. W.; Schleyer, P. v. R. *J. Comput. Chem.* **1983**, *4*, 294–301. (b) Frisch, M. J.; Pople, J. A.; Binkley, J. S. *J. Chem. Phys.* **1984**, *80*, 3265–3269.
- (59) (a) Head-Gordon, M.; Pople, J. A.; Frisch, M. J. *Chem. Phys. Lett.* **1988**, *153*, 503–506. (b) Frisch, M. J.; Head-Gordon, M.; Pople, J. A. *Chem. Phys. Lett.* **1990**, *166*, 275–280. (c) Frisch, M. J.; Head-Gordon, M.; Pople, J. A. *Chem. Phys. Lett.* **1990**, *166*, 281–289. (d) Head-Gordon, M.;

Head-Gordon, T. *Chem. Phys. Lett.* **1994**, *220*, 122–128. (e) Pople, J. A.; Krishnan, R.; Schlegel, H. B.; Binkley, J. S. *Int. J. Quantum Chem.* **1979**, *13*, 325. (f) Handy, N. C.; Schaefer, H. F., III. *J. Chem. Phys.* **1984**, *81*, 5031–5033.

(60) (a) Barone, V.; Cossi, M. *J. Phys. Chem. A* **1998**, *102*, 1995–2001. (b) Cossi, M.; Rega, N.; Scalmani, G.; Barone, V. *J. Comput. Chem.* **2003**, *24*, 669–681.

(61) *Handbook of Chemistry and Physics*, 83rd ed.; Lide, D. R., Ed.; CRC Press: Boca Raton, FL, 2002–2003; pp 7–1, and references therein.